Microflanging of CuZn30 Specimens Using Electromagnetic Forming

R. VanBenthysen[1] and B. L. Kinsey[1]

[1]Mechanical Engineering Department, University of New Hampshire. Durham, NH, USA

Abstract

In this research, electro-magnetic (EM) forming was investigated as an alternative process to form microscale components. Both EM and quasi-static flanging experiments were conducted with CuZn30 specimens of 0.127, 0.508 and 1.588 mm thicknesses that were heat treated to achieve 2 and 10 grains through the thickness to assess this parameter. Results from the quasi-static tests showed that as the sample size decreased with a constant grain size through thickness ratio, the springback angle increased. For the 0.127mm and 0.508mm thickness specimens, the EM results showed that the flanging angle increased as the power input increased from 1.7 to 3.7 kJ. For 3.7 kJ energies and above, complete 90 degree flanging with no springback was achieved for the 0.508mm specimens. However, EM flanging could not be achieved for the 1.588mm case. Microhardness testing conducted on specimens of similar flanging angles yielded no observable change in deformation between the EM and quasi-static processes for the 0.508mm specimens.

Keywords

Forming, Miniaturization, Springback

1 Introduction

Recently there has been an increasing trend towards miniaturized systems, e.g., smart phones, mp3 players, personal computers, sensors, etc. An estimated 1.8 billion MEMS devices were shipped in 2005, with an anticipated growth of 11% through 2010 [1]. An increasing number of industries utilize these miniaturized systems including automotive, electronics, medical, defense and aerospace. With the increase in these systems comes the need to manufacture them in a more efficient, cost effective, and repeatable manner. Since macroscale manufacturing processes cannot be scaled down to produce these miniaturized components, alternative methods such as microinjection molding, micromachining, IC processing and microforming are used. Microforming is a high rate, cost effective process that involves plastically deforming components with at least two sub millimeter dimensions [2].

The inability to scale down conventional manufacturing processes stems from size effects, i.e. variations in material properties and process parameters as the grain size approaches the specimen feature size [3]. The results are anomalies in final part shapes, springback, increased data scatter, variations in frictional effects, etc. An example of a shape anomaly can be seen in Figure 1 as the pin with a coarse grain size of 211µm curves after being extruded from .76mm to .57mm [4]. This was caused by the size and orientation of a single grain in the material. A macroscale component generally consists of many grains through a thickness or part feature whereas a microscale component may consist of only a few grains and possible less than a single grain. Figure 2 demonstrates the effects of varying the number of grains through the thickness (φ) on yield strength during bending and tensile tests [5]. It can be seen that as φ is reduced from 10 to 1, there is a decrease in yield strength associated with an increased ratio of surface to volume grains [2]. As φ is decreased further, the yield strength increases due to the effect of individual grain orientation. In addition, a decrease in the φ also causes an increase in data scatter.

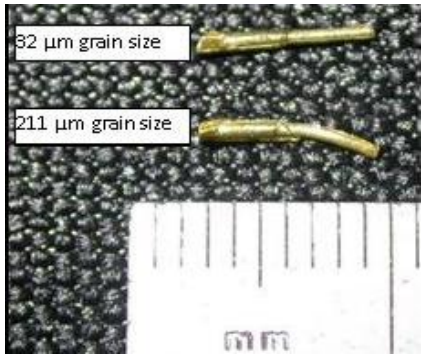

***Figure 1** : Shape anomaly due to miniaturization of micro-extruded pins [4]*

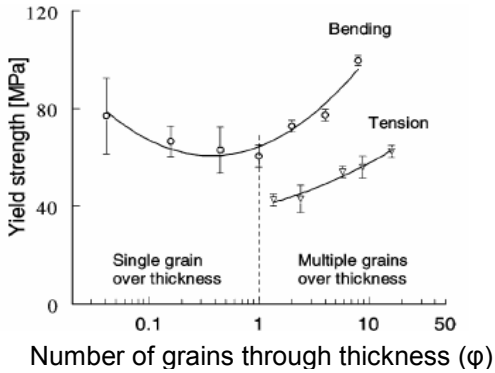

***Figure 2** : Effect of miniaturization during bending and tensile tests [5]*

For bending processes, springback and data scatter are of utmost concern. The inability to predict final part geometry would significantly reduce the consistency of manufacturing. Figure 3 demonstrates how springback is affected by miniaturization of the feature. In this case, a scaling factor λ is introduced to specify the geometry scaling [6]. Al 99.5 was used in the experiments and a λ of 1 corresponds to 200µm thickness. The three grain sizes presented all show the effect of an increased springback angle as the scaling factor is decreased.

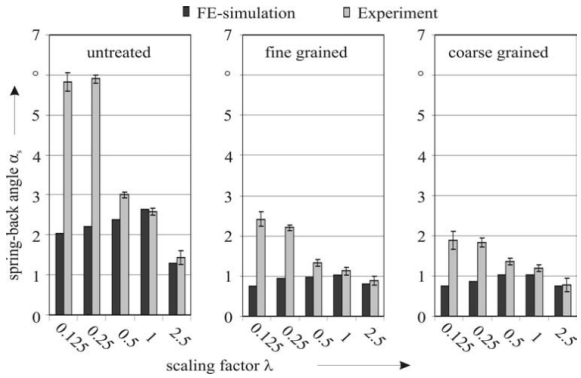

***Figure 3** : Effect of miniaturization on springback angle and data scatter during bending [6]*

In this paper, results from both EM and quasi-static flanging experiments are presented. As in past research, the springback angle increased with miniaturization for quasi-static experiments. The EM flanging process was able to achieve no springback (i.e. 90 degree flanging) for the 0.588mm and 0.127mm cases. The quasi-static case was unable to achieve 90 degree flanging due to springback and limitations of the die and punch setup. Microhardness measurements performed on both quasi-static and EM flanged specimens did not reveal any significant difference in deformation. Finally, simulations were conducted to design an EM flanging coil for future bending experiments.

2 Quasi-static Setup

The quasi-static and EM flanging processes utilized dies and punches with features that were a function of the specimen's thickness. CuZn30 specimens (0.127, 0.508 and 1.588mm thicknesses) were used. Figures 4 and 5 show schematics of the sample and tooling. To achieve a plane strain condition the sample width was ten time the thickness (10t). Sample lengths were twenty six times the thickness (26t) to assure contact between the sample and punch at full punch depth. Heat treatments were used to achieve a desired 2 and 10 grains through the thickness for all three specimen sizes (see Table 1). These values were chosen as it is estimated that size effects will arise when less than 15 grains through a feature size are present [7]. See [8] for further details and results related to the quasi-static experiments.

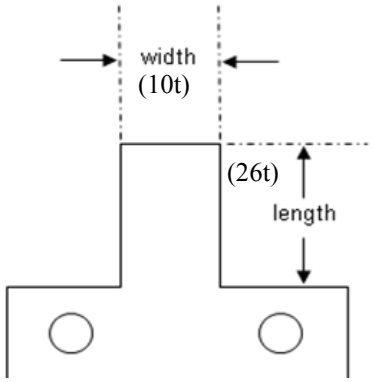

Figure 4 *: Schematic of Sample*

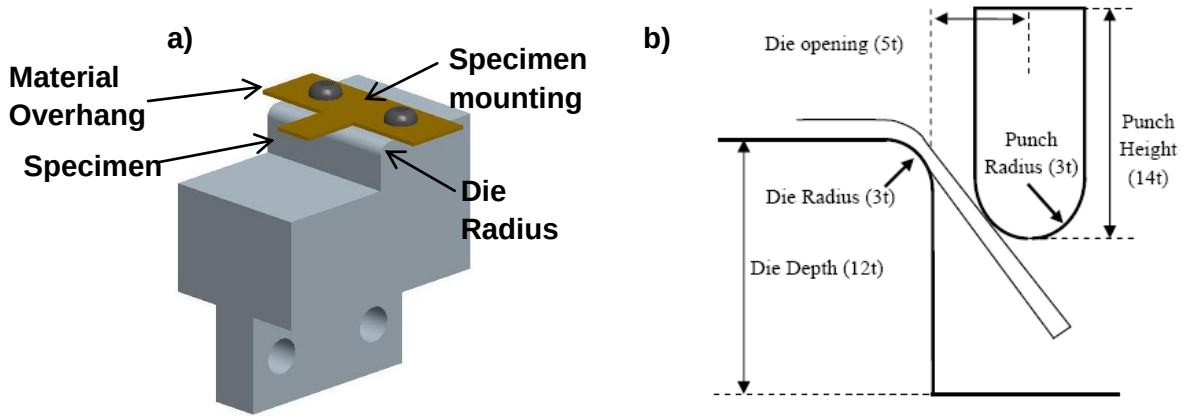

Figure 5 *: Schematic of a) Sample and Die combination and b) tooling features bases on specimen thickness*

Thickness (μm)	Target grains through thickness	Measured grain size (μm)	Measured grains through thickness	Heat Treatment (degrees C)	Duration (minutes)
1588	2	484.4	3.1	800	90
	10	127.5	11.8	665	90
508	2	208.3	2.4	700	60
	10	45.5	11	600	60
127	2	55.2	2.3	800	75
	10	15.0	8.5	600	60

Table 1 *: Heat treatment information and achieved grain sizes for various sheet thicknesses.*

3 Quasi-static Springback Results

For a similar number of grains through the thickness, the springback angle increased as the sample size decreased (see Table 2). This was measured optically using digital images and software. At the desired depth a picture was taken with the punch still in contact with the specimen. The punch was then removed and another picture was taken. These two images were then compared to determine the springback angle as can be seen in Figure 6.

a)

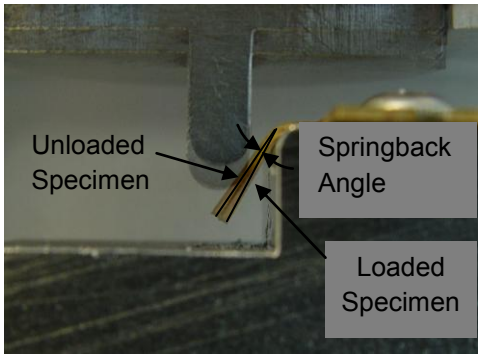

Figure 6 *: Springback in 0.508mm specimen*

b)

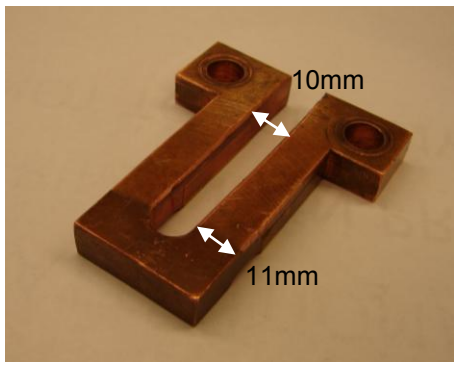

Figure 7 *: Cu101 coil*

sample #	Sample size (μm) / # of grains through thickness					
	127 / 10	127 / 2	500 / 10	500 / 2	1500 / 10	1500 / 2
1	4.6	4	3.3	2.3	1.8	2.9
2	3.3	4.4	4.4	1.4	1.6	1.8
3	2.9	4.4	3.8	2	1.8	2.2
4	5.4	3.7	3	2.2	2.2	1.4
5	4.6	4.1	3.1	-	2.9	1.6
average	4.16	4.12	3.52	1.975	2.06	1.98

Table 2 *: Springback angle values in degrees for various cases*

4 EM Flanging Experimental Setup

The dies used in the quasi-static process were also used for the EM flanging while the punch force is replaced by the force resultant of the magnetic field. A Cu101 coil for EM flanging was designed by Hirotec inc., a collaborator on this project. The coil and its location above the sample are shown in Figures 7 and 8 respectively. The specimen positioning on the die can be seen in Figure 5a.

The EM flanging setup is shown in Figure 9. The steel plates attached with bolts are to prevent unwanted deformation in the coil's leads, as the magnetic field that forms the specimen also affects the opposing lead of the coil. Kapton tape was used to prevent arcing between adjacent metal surfaces. The die is placed in a piece of G10 for easy positioning.

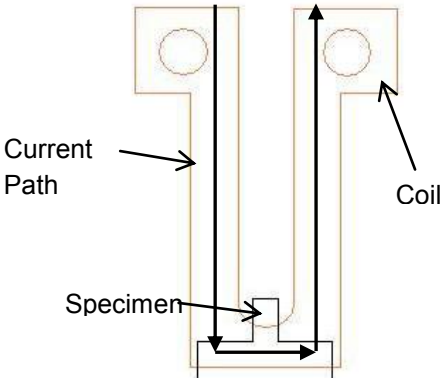

Figure 8 *: Position of sample under coil*

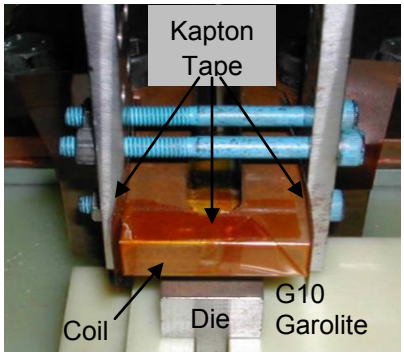

Figure 9 *: EM Flanging setup at Hirotec Inc.*

5 EM Flanging Experimental Results

For the 0.127mm and 0.508mm cases, the input energy level was varied in order to determine its effect on the flanging angle. The effect of the input energy on the 0.508mm specimens is shown in Figure 10 and Table 3. As expected, the flanging angle increases with increased energy input. Complete flanging was achieved for energy levels above 3.7 kJ. Since the distance between the coil legs (10mm, see Figure 7) is less than the 1.588mm specimen width (15.88mm), flanging was not achieved on the outer edges for this specimen (see Figure 11). This may be due to the repulsive eddy currents only being produced in the specimen's center as will be discussed in the section on coil design. Also, the energy level used may not have been sufficient for the deformation even if a wider coil width was used.

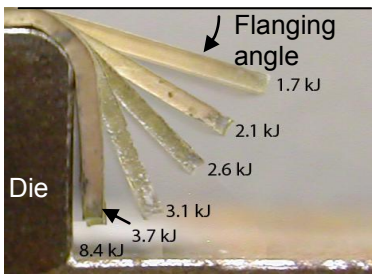

Figure 10 *: Effect of energy input on flanging angle for 0.508mm specimen*

Figure 11 *: EM Non uniform flanging of 1.588mm specimen.*

0.5 mm specimens		
Input energy setting (kJ)	Flanging angle in degrees	
	10 grains/thickness	2 grains/thickness
1.7	23.8	17.4
2.1	30.6	32.0
2.6	47.7	47.3
3.1	58.5	67.9
3.7	87.3	86.5
4.4	87.2	87.0
5.1	86.3	87.1
6.6	86.2	86.4
8.4	86.6	86.8

***Table 3** : Comparison of flanging angles and grain size ratios for various energy inputs*

Complete flanging of the 0.127mm specimen was also achieved with an energy level of 3.1kJ (see Figure 12). However, a driver material was required for the 0.127mm case which is in agreement with skin depth calculations performed to determine the minimum thickness required to achieve EM flanging (i.e., 0.328mm) [8]. Note though that the ends of the mounting strip (which were larger than the specimen and hung over the sides of the die; see Figure 5a) were flanged despite not having the driver material in this area. See Figure 12. Thus the effectiveness of flanging is affected by the area (length x width) as well as the thickness. This may be due to the eddy currents not being generated in the small specimen area of our workpiece. Effective design of a coil is needed to correct this concern.

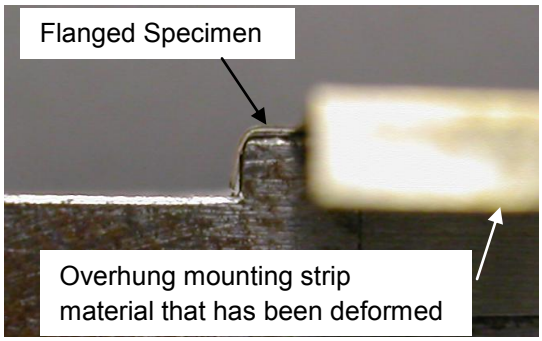

***Figure 12** : Complete flanging of 0.127mm specimen*

Hardness measurements through the thickness and along the bent region were obtained in order to observe any difference in the deformation mechanism inherent to each process. Since EM flanging was not achieved with the 1.588mm specimens and microhardness indentations are too large to produce sufficient data for the 0.127mm specimens, only hardness measurements on the 0.508mm specimens were conducted. An EM flanged specimen (3.1kJ) with a similar angle to the quasi-static case was chosen for comparison. Figure 13 shows the hardness contour plots for these cases. Hardness

measurements were also taken for the complete flanging case (3.7kJ). See Figure 14. The hardness profiles shown cover the whole bent region of the deformed specimens with a zero position along the length corresponding to the start of the die radius and the zero position through the thickness corresponding to the mid-plane of the sheet.

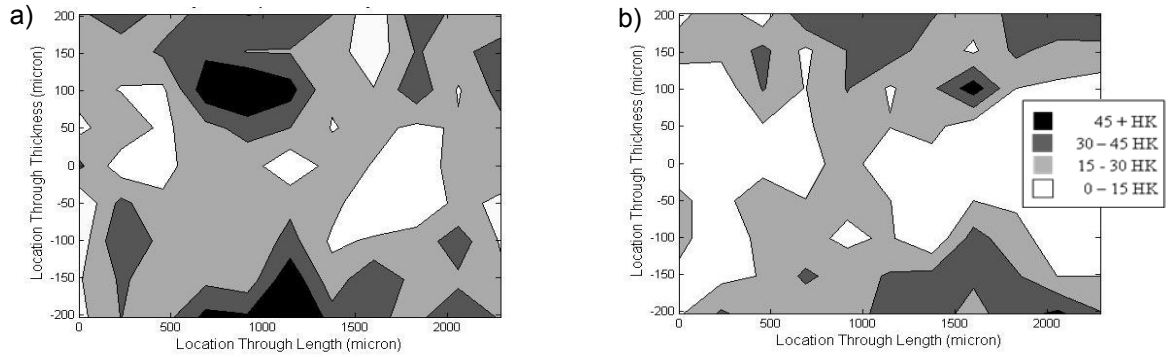

***Figure 13** : Contour plots for the a) quasi-static and b) EM processes, both 10 grains/thickness*

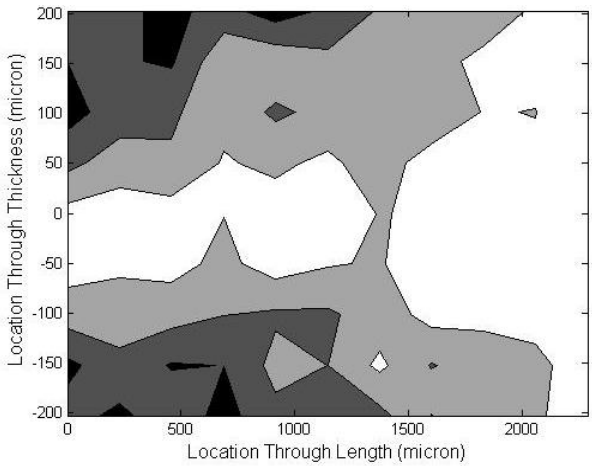

***Figure 14** : Hardness plot for 3.7kJ, 10 grains/thickness*

Comparing the quasi-static and 3.1kJ cases, there is no change in deformation present. The plots show a rough layered pattern with higher hardness at the surface of the sheet and lower hardness near the neutral axis. This rough pattern is due to only one set of measurements being taken. Only one sample was EM flanged for every thickness and grain size ratio; thus, obtaining an average plot is not possible. However, past three point bending research utilizing the same punches and dies with features based on the same specimen thickness ratio has shown an increased definition in hardness layering when an average plot is obtained. See Figure 15. An average of four samples (see Figure 15b) shows a much more defined hardness layering pattern than that of only one sample (see Figure 15a). The 3.7kJ case demonstrates more of a layered pattern due to the increased strain from a larger amount of deformation. Note that the plots in Figures 13-15 are the increase in hardness from the center region.

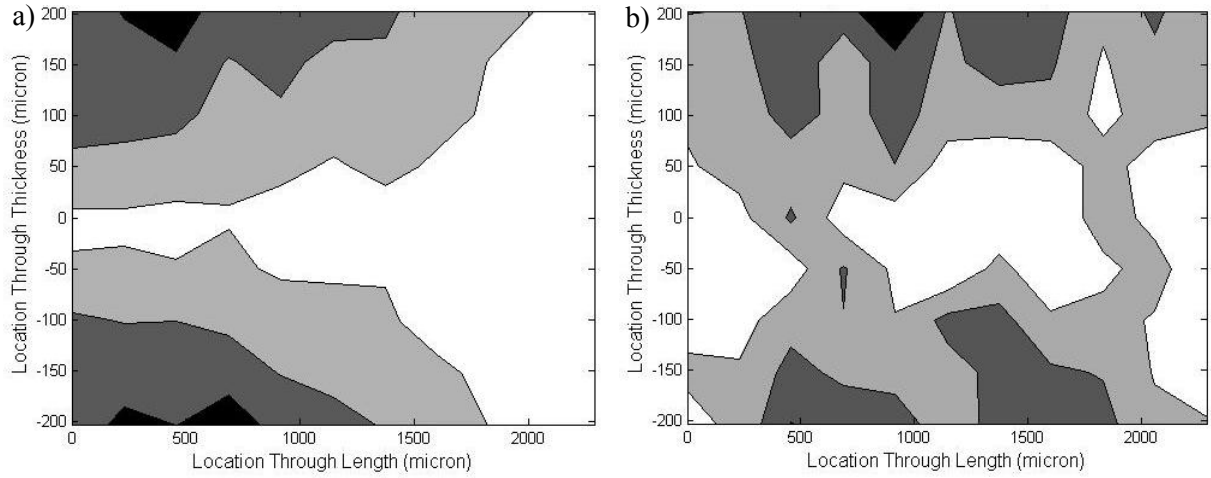

***Figure 15** : Results from past 3 point bending experiments. a) 1 set or measurements and b) an average of 4 sets*

6 Coil Design Simulations

In order to continue this research, a Magneform JA7000 series 12kJ machine, which is capable of producing a 400kA current with 6000V, was acquired. As the largest sample was unable to be uniformly EM flanged (see Figure 11), a coil for this specific specimen will be designed and fabricated. To avoid unwanted deformation of the coil legs, a single leg coil will be utilized (see Figure 16). Various designs were modeled in Magnet, an electromagnetic simulation package by Infolytica Corp. To compare magnitudes and uniformity of the magnetic fields, static cases were conducted. Of course, EM forming is a dynamic process; however, it was anticipated that these static cases would provide reasonable results with respect to the differences in coil geometries. Since only one leg of the coil is of concern, the model was a 2-D representation of the cross-section. See Figure 17 for the four different geometries. A current of 146kA was used due to an assumed rise time of 10μs. The coil material used is Cu101. The bottom face of the coil (19mm) was designed to be larger than the width of the large specimen (15.88mm). This is to assure that the specimen experiences a more uniform magnetic field. See Figure 17d for this length (L).

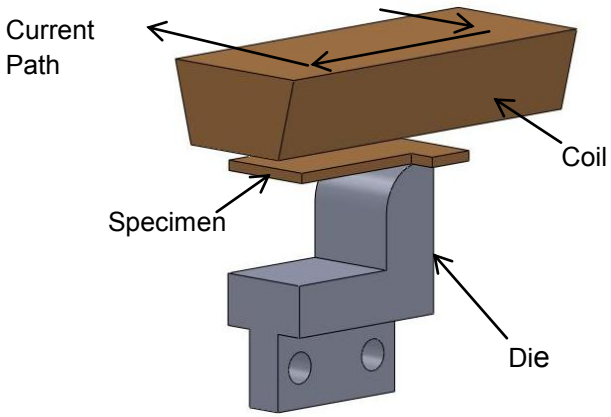

***Figure 16** : Schematic of single turn coil, die and specimen*

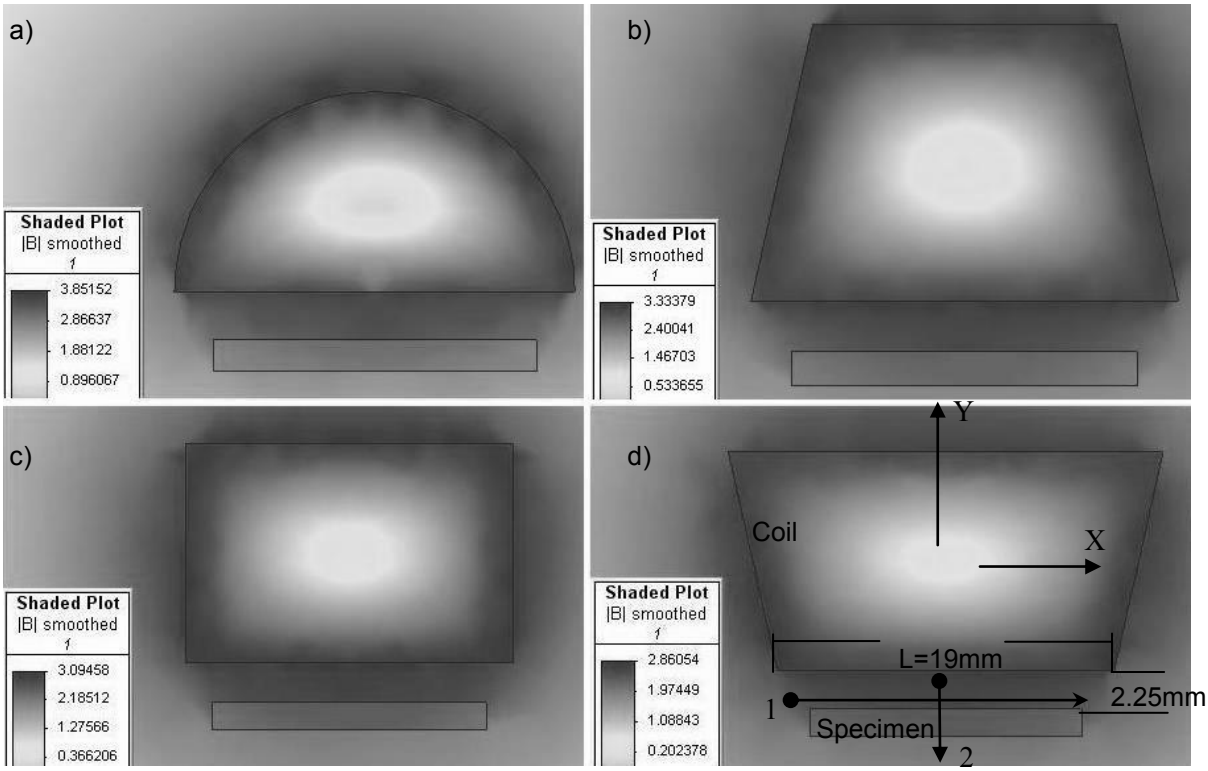

***Figure 17** : Different coil models for EM flanging; A) semi circular, B) inward 15º taper, C) rectangular and D) outward 15º taper. The units of B (the magnetic flux density) are Tesla.*

Line plots of the magnetic field were obtained for each coil design; 1) Along the width of the specimen at a distance of 2mm under the coil face and 2) from the bottom of the coil through the specimen thickness, at the vertical midplane of the coil (X=0). See Figure 17d for a visual representation of these two directions. Data for the 1 and 2 directions are shown in Figure 18. Figure 18b shows the effect of the specimen on the magnetic field's magnitude.

The coils were designed so the cross-sectional areas increase from geometry A to geometry D. Thus the current density is decreased and a lower magnetic field value (B) is predicted. However, lower B values also correlate to a more consistent magnetic field across the width of the specimen (see Figure 18a). This is desirable since a lower consistency may lead to non-uniform flanging, as was the case in past experiments with the largest specimen (1.588mm) (see Figure 11). Since previous experiments suffered from the lack of a uniform magnetic field, geometry D (outward taper) was chosen as it has the most uniform magnetic field across the width of the sample (from approximately -8mm < X < 8mm). Note the specimen may be located directly under the coil or may be offset. This will be adjusted to produce eddy currents that flow in a circular pattern in order to produce an optimal repulsive magnetic force for forming.

7 Conclusions

Increased springback was observed for a decrease in sample size with a similar number of grains through the thickness (φ) in our quasi-static microscale experiments. No change in hardness was observed for EM and quasi-static specimens of similar flanging angle. The

0.127mm and 0.508mm specimens experienced near complete flanging angles for power levels at approximately 4kJ. The 1.588mm specimen was unable to achieve a uniform flange due to the size of the coil in relation to the specimen's width. A new EM coil design for flanging of the 1.588mm thickness specimens was investigated.

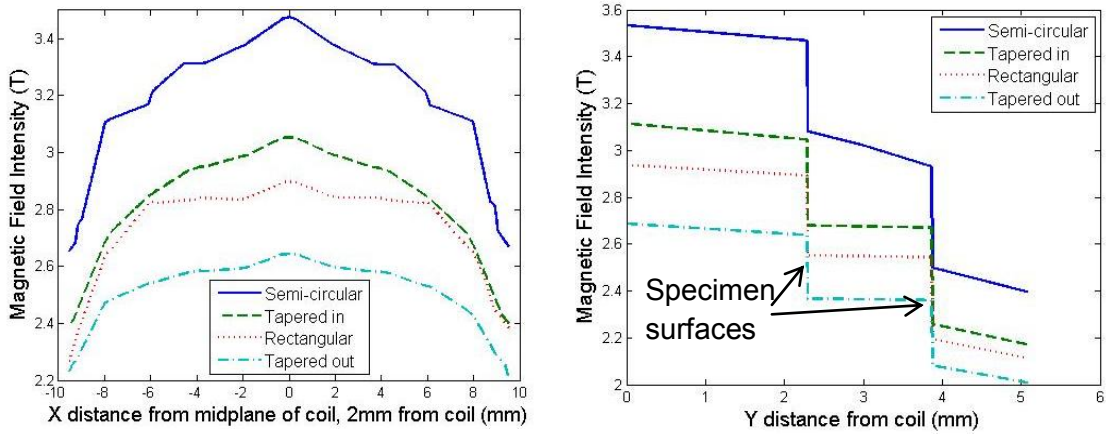

***Figure 18** : Plots of magnetic field intensity versus location a) along and b) perpendicular to the specimen for various coil geometries*

.Acknowledgments

Funding from the National Science Foundation (CMMI-0644705) and assistance with the EM flanging experiments from Hirotec America, Inc. are gratefully acknowledged

References

[1] In-Stat, "An Industry in Transition: 2006 MEMS Forecast", IN0603149ESCA, 2006.
[2] Geiger, M., Kleiner, M., Eckstein, R., Tiesler, N. and Engel, U., "Microforming", Keynote Paper, *Annals of the CIRP*, 50-2, 2001, 445-462.
[3] Armstrong R.W., "On Size Effects in Polycrystal Plasticity," *J. Mechanics & Physics of Solids*, 9, 1961, 196-199.
[4] Parasiz, S., VanBenthysen, R., and Kinsey, B.L., "Deformation Size Effects Due to Specimen and Grain Size in Microbending", *Journal of Manufacturing Science and Engineering*, 132, 2010, in press.
[5] Raulea, L.V., Goijaerts, A.M., Govaert, L.E., and Baaijens, F.P.T., "Size effects in the processing of thin metal sheets", *J. of Mat. Processing Technology*, 115, 2001, 44-48.
[6] Diehl, A., Engel, U., and Geiger, M., "Investigation of the spring-back behavior in metal foil forming", *Proceedings of the 24th IDDRG Conference*, Besancon, Frankreich, 2005.
[7] Hansen, N., "The effect of grain size and strain on the tensile flow stress of Aluminum at room temperature", *Acta Metallurgica*, 25, 1971, 863-869.
[8] VanBenthysen et al., "Comparison of Microscale Flanging Using Quasi-Static and Electromagnetic Forming Processes", *2008 International Manufacturing and Science Engineering Conference (MSEC),* Evanston, IL, Oct. 8-10, 2008.